

High Affinity Central Benzodiazepine Receptor Ligands. Part 2: Quantitative Structure–Activity Relationships and Comparative Molecular Field Analysis of Pyrazolo[4,3-*c*]quinolin-3-ones

L. Savini,^b L. Chiasserini,^b C. Pellerano,^b G. Biggio,^c E. Maciocco,^c
M. Serra,^c N. Cinone,^{a,d} A. Carrieri,^a C. Altomare^a and A. Carotti^{a,*}

^aDipartimento Farmaco Chimico, Università degli Studi, via E. Orabona 4, I-70125 Bari, Italy

^bDipartimento Farmaco Chimico Tecnologico, Università degli Studi, A. Moro, I-53100 Siena, Italy

^cDipartimento di Biologia Sperimentale, via Palabanda 12, Università degli Studi, I-09123 Cagliari, Italy

^dDipartimento di Scienze del Farmaco, Università degli Studi “G. D’Annunzio”, via dei Vestini 31, I-66013 Chieti Scalo (CH), Italy

Received 17 July 2000; accepted 26 September 2000

Abstract—A large series of 2-aryl(heteroaryl)-2,5-dihydropyrazolo[4,3-*c*]quinolin-3(3*H*)-ones (PQ, 106 compounds), carrying appropriate substituents at the quinoline and N₂-phenyl rings, were designed, prepared and tested as central benzodiazepine receptor ligands. Compounds with an affinity significantly higher than the parent compound CGS-8216 were obtained, the most active ligand showing a pIC₅₀ = 10.35. Hansch and comparative molecular field analyses gave coherent results suggesting the main structural requirements of high receptor binding affinity. The possible formation of a three-centred hydrogen bond (HB) at the HB donor site H₂, as a key interaction for high receptor binding affinity, was assessed by the calculation and comparison of the molecular electrostatic potentials of a series of selected ligands. © 2001 Elsevier Science Ltd. All rights reserved.

Introduction

Benzodiazepine receptor (BzR) ligands are structurally diverse compounds that bind to the GABA_A/BzR complex evoking numerous neurological effects including convulsion, anxiety and sleep, and influencing memory and learning processes.^{1–3}

The GABA_A/BzR complex contains a chloride channel and it is a membrane-bound heteropentameric protein composed principally of α , β , and γ subunits. Presently, a total of 21 subunits (6 α , 4 β , 4 γ , 1 ϵ , 1 δ , 3 ρ , 1 θ , and 1 π) of the GABA_A receptor have been identified by molecular cloning⁴ and 16 of them have been found in the mammalian CNS.⁵ It has been found that a functional GABA_A/BzR must contain α , β , and γ subunits. The heterogeneity of GABA_A/BzR subtypes has been indicated as the main factor responsible for the multiplicity of the pharmacological properties displayed by benzodiazepines but no clear and definitive link of the observed pharmacological activities to the diverse receptor sub-

types has been identified yet.⁶ Recent evidence suggests that subtype receptors with $\alpha_1\beta_2\gamma_2$ subunit combinations show many of the pharmacological effects associated with the type I BzR, whereas $\alpha_2\beta_2\gamma_2$, $\alpha_3\beta_2\gamma_2$ and $\alpha_5\beta_2\gamma_2$ subunit compositions characterise the biological effects of the so called type II BzR.⁷

The possibility to carry out nowadays binding and pharmacological studies on cloned BzR subtypes with a well defined subunit composition should lead to a better understanding of which subtypes mediate which specific physiological response(s). Unfortunately, highly potent and subtype-selective ligands, designed on the basis of SAR studies on cloned receptor subtypes with well defined subunit combinations, did not show the expected pharmacological profile.⁸

While this new approach seems very rational and promising, these initial discouraging results demonstrate that there is still a long way ahead to reach a better comprehension of the structure–function relationships of the diverse BzR subtypes.

In this context, research based on traditional binding affinity and intrinsic efficacy studies can still play a role

*Corresponding author. Tel.: +39-080-544-2782; fax: +39-080-544-2230; e-mail: carotti@farmchim.uniba.it

to improve our knowledge on the main structural requirements necessary for a high binding affinity and possibly a well defined intrinsic activity.^{9–14} Indeed, several pharmacophore models proved useful for the design of new and potent BzR ligands.¹⁵ In this field, a significant contribution also came from 2-D and 3-D QSAR studies^{16,17} on a new class of BzR ligands, the 2-aryl-2,5-dihydropyridazino[4,3-*b*]indol-3(3*H*)-ones and from a preliminary 2-D QSAR study¹⁸ on a structurally related class of ligands, the well known 2-aryl-2,5-dihydropyrazolo[4,3-*c*]quinoline-3(3*H*)-ones (PQs).¹⁹

PQs constitute a biologically interesting class of BzR ligands because of their peculiar pharmacological activity, lacking many unwanted side effects observed in classical benzodiazepines. Moreover, the net shift of intrinsic activity, from agonist, through antagonist, to inverse agonist, caused by small structural modifications of PQs render this class of compounds particularly appealing for deep structure–efficacy relationship studies.^{20–24} Finally, PQs represent ideal model compounds to carry out SAR investigations in that they can be easily prepared through simple and well consolidated synthetic methods,^{25,26} thus allowing a proper exploration of their physicochemical and structural properties.

A preliminary account of a QSAR study of PQs has been recently reported by us in this journal.¹⁸ In the present paper, we describe the design, synthesis, 2-D and 3-D QSAR studies of a further set of PQ BzR ligands. The molecular skeleton of PQs was appropriately substituted aiming at the identification of the primary ligand–receptor interactions, all around the quinoline and the N₂-phenyl rings, responsible for recognition and different activation of BzR. To reach this important objective, a high number of PQ analogues (listed in Table 1) were synthesised and their BzR affinity measured by radioligand binding assay. In particular, several mono- and polysubstituted derivatives at the quinoline ring and monosubstituted *ortho*, *meta*, and *para* congeners at the N₂-phenyl ring were prepared. The aryl substituents at position 2 were also replaced by nitrogen heterocycles. The overall structural modifications were such that the substituent physicochemical space was more thoroughly explored for *meta* and *para* congeners and for positions 6, 7, and 8 of the quinoline moiety.

Our main goals were to reinforce and complement our previous SAR and QSAR results and to derive meaningful and highly predictive 3-D QSAR models, by means of Comparative Molecular Field Analysis (CoMFA). The development of significant structure–efficacy relationship (SER) models is also being pursued by analysing intrinsic activity data of a properly selected set of PQ ligands, measured through a binding assay with [³⁵S]TBPS,^{27,28} and an electrophysiological assay on the cloned receptor subtype $\alpha_2\beta_2\gamma_2$. The results from this SER study will be reported soon in this journal.

It is worth underlining that, with the only exception of compounds **2**₂ and **2**₆, all the binding data reported in Table 1 have been measured by the same method and in the same laboratory and therefore are very homogeneous

and well suited to perform QSAR studies. In addition the examined data set covers a wide range of activity spanning quite regularly more than four orders of magnitude intervals.

Chemistry

The general synthetic procedure to prepare the pyrazolo[4,3-*c*]quinoline derivatives (**2**) is shown in Scheme 1.

Compounds **2** were obtained according to previously described methods¹⁸ by reacting ethyl-4-chloroquinoline-3-carboxylates (**1**) with substituted phenylhydrazines or α -(*N*)-heterocyclhydrazines.

All the synthesised PQs were isolated in satisfactory yields (40–60%). Their spectral data (IR and ¹H NMR) are in accordance with literature¹⁹ data and allow unequivocal structural assignments to all new compounds. In the ¹H NMR spectra, the characteristic signals for PQs (**2**) were a singlet between 8.4 and 8.9 δ , attributable to H-4 proton, and a broad singlet, exchangeable with D₂O, between 12.3 and 13.2 δ due to the N₅-H proton. Due to a possible tautomeric equilibrium, sometimes the H-4 proton appeared as a doublet and collapsed to a singlet upon treatment with D₂O (see compound **2**₈₁). In Table 2, the IR and ¹H NMR spectral data of some representative PQs are reported.

The known compounds CGS-8216 and CGS-9896 were also synthesised as biological standards. Their physical and spectral properties are consistent with literature values.²⁰

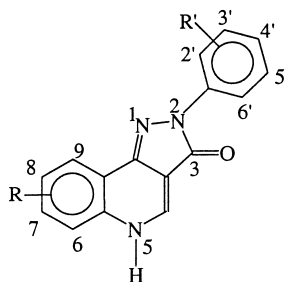
The hydroxy derivatives **2**₂₃, **2**₃₆, **2**₃₇ and **2**₇₇ were conveniently obtained from the corresponding alkoxy derivatives by hydrolysis with 48% HBr in glacial acetic acid. Catalytic reduction with 10% Pd/C of nitro compounds **2**₅, **2**₈, **2**₂₁ and **2**₈₀ afforded the target amino derivatives **2**₄, **2**₇, **2**₂₂ and **2**₇₉, as already described.¹⁸

Compounds **2**₁₀₁ and **2**₁₀₂ were prepared from the corresponding chloro derivatives (**1a** and **1b**) and phenylhydrazine in analogy with all other described PQs (**2**). The dimethylamino derivative **2**₇₁ was obtained by reductive methylation of the corresponding amino derivative **2**₆₈ with formaldehyde, on Pd/C.

Compound 8-trifluoromethoxy-2-(4-hydroxy-3-nitrophenyl) pyrazolo[4,3-*c*]quinolin-3-one was synthesised by nitration of 8-trifluoromethoxy-2-(4-hydroxyphenyl) pyrazolo[4,3-*c*]quinolin-3-one¹⁸ using KNO₃, aqueous sulfuric acid and a catalytic amount of sodium nitrite; its subsequent catalytic reduction with 10% Pd/C yielded the corresponding amino derivative **2**₇₃.

Biochemistry

The compounds listed in Table 1 were tested for their ability to displace [³H]flunitrazepam binding from rat brain membranes according to standard procedures.³⁴

Table 1. Chemical structures and binding affinities of pyrazolo[4,3-*c*]quinolin-3-ones (**2**₁–**2**₁₀₇)

Compound	R ₆	R ₇	R ₈	R ₉	R _{6'(2')}	R _{5'}	R _{4'}	pIC ₅₀ ^a	Mp (°C) ^b	Cryst. solvent ^c
2 ₁ ^d	H	H	H	H	Unsubstituted at N2			6.30	> 300	A
2 ₂ ^{e,f}	H	H	H	H	H	H	H	9.35	—	—
2 ₃ ^f	H	H	H	H	H	Cl	H	8.16	—	—
2 ₄	H	H	H	H	H	NH ₂	H	9.77	> 300	A
2 ₅	H	H	H	H	H	NO ₂	H	8.53	> 300	D
2 ₆ ⁿ	H	H	H	H	H	H	OH	9.40	> 300	A
2 ₇ ⁿ	H	H	H	H	H	H	NH ₂	8.67	> 300	A
2 ₈ ⁿ	H	H	H	H	H	H	NO ₂	7.96	> 300	A
2 ₉ ^{e,f}	H	H	H	H	H	H	Cl	9.00	—	—
2 ₁₀ ^{e,f}	H	H	H	H	H	H	OCH ₃	9.17	—	—
2 ₁₁ ^{f,g}	H	H	H	H	H	H	H	6.84	—	—
2 ₁₂ ^{f,g}	H	H	H	H	H	H	Cl	6.75	—	—
2 ₁₃ ^h	F	H	H	H	H	H	H	8.16	> 300	A
2 ₁₄ ^l	CH ₃	H	H	H	H	H	H	7.18	> 300	A
2 ₁₅ ^h	CF ₃	H	H	H	H	H	H	5.73	294–296	B
2 ₁₆ ^l	OCH ₃	H	H	H	H	H	H	5.66	288–290	A
2 ₁₇ ^f	H	OCH ₃	H	H	H	H	H	8.37	> 300	A
2 ₁₈ ^m	H	Cl	H	H	H	H	H	8.67	> 300	A
2 ₁₉	H	F	H	H	H	H	H	9.01	> 300	A
2 ₂₀ ^m	H	CF ₃	H	H	H	H	H	7.64	> 300	A
2 ₂₁	H	NO ₂	H	H	H	H	H	7.69	> 300	C
2 ₂₂	H	NH ₂	H	H	H	H	H	8.86	285–288	B
2 ₂₃	H	OH	H	H	H	H	H	8.88	> 300	A
2 ₂₄ ⁿ	H	H	F	H	H	H	H	9.54	> 300	A
2 ₂₅ ^h	H	H	F	H	H	NO ₂	H	8.70	> 300	D
2 ₂₆ ^h	H	H	F	H	H	NH ₂	H	9.26	> 300	A
2 ₂₇ ⁿ	H	H	F	H	H	H	OCH ₃	9.48	290 (dec)	A
2 ₂₈ ^h	H	H	F	H	H	H	OH	9.34	> 300	A
2 ₂₉ ^e	H	H	Cl	H	H	H	H	9.37	—	—
2 ₃₀	H	H	Cl	H	2-Pyrid-2'-yl			9.37	> 300	E
2 ₃₁ ^e	H	H	OCH ₃	H	H	H	H	9.17	—	—
2 ₃₂	H	H	OCH ₃	H	F	H	H	8.80	> 300	A
2 ₃₃	H	H	OCH ₃	H	2-Pyrimid-2'-yl			7.75	> 300	B
2 ₃₄ ^h	H	H	OC ₂ H ₅	H	H	H	H	8.85	> 300	B
2 ₃₅	H	H	OC ₂ H ₅	H	H	H	Cl	8.56	> 300	A
2 ₃₆	H	H	OH	H	H	H	H	9.70	> 300	A
2 ₃₇	H	H	OH	H	H	H	Cl	9.28	250 (dec)	E
2 ₃₈ ⁱ	H	H	<i>n</i> -C ₄ H ₉	H	Unsubstituted at N2			6.30	—	—
2 ₃₉ ^j	H	H	<i>n</i> -C ₄ H ₉	H	H	H	H	9.00	—	—
2 ₄₀	H	H	<i>n</i> -C ₄ H ₉	H	F	H	H	9.18	240–243	A
2 ₄₁ ^h	H	H	<i>n</i> -C ₄ H ₉	H	H	H	COOH	5.93	> 300	E
2 ₄₂	H	H	<i>n</i> -C ₄ H ₉	H	H	H	COOCH ₃	6.86	286 (dec)	A
2 ₄₃ ^h	H	H	<i>n</i> -C ₄ H ₉	H	2-Pyrid-2'-yl			9.50	263–267	B
2 ₄₄ ^h	H	H	<i>n</i> -C ₄ H ₉	H	2-Pyrimid-2'-yl			8.77	> 300	A
2 ₄₅ ^h	H	H	<i>n</i> -C ₄ H ₉	H	2-Pyrazin-2'-yl			9.22	270 (dec)	B
2 ₄₆ ^j	H	H	<i>c</i> -C ₆ H ₁₁	H	H	H	H	8.35	—	—
2 ₄₇ ^h	H	H	<i>c</i> -C ₆ H ₁₁	H	H	H	COOH	5.55	> 300	A
2 ₄₈ ^h	H	H	<i>c</i> -C ₆ H ₁₁	H	2-Pyrid-2'-yl			8.60	> 300	A
2 ₄₉ ^h	H	H	<i>c</i> -C ₆ H ₁₁	H	2-Pyrimid-2'-yl			8.36	> 300	C
2 ₅₀ ^h	H	H	<i>c</i> -C ₆ H ₁₁	H	2-Pyrazin-2'-yl			8.16	> 300	B
2 ₅₁ ^f	H	H	OBn	H	H	H	H	7.75	—	—
2 ₅₂ ^h	H	H	OCF ₃	H	Unsubstituted at N2			6.94	> 300	B
2 ₅₃ ^h	H	H	OCF ₃	H	H	H	H	9.15	> 300	A
2 ₅₄ ^h	H	H	OCF ₃	H	F	H	H	9.40	268–271	F
2 ₅₅ ^h	H	H	OCF ₃	H	Cl	H	H	8.60	291–294	B
2 ₅₆ ^h	H	H	OCF ₃	H	CH ₃	H	H	8.47	290–292	B
2 ₅₇ ^h	H	H	OCF ₃	H	H	Br	H	7.46	> 300	A
2 ₅₈ ^h	H	H	OCF ₃	H	H	CH ₃	H	8.20	295 (dec)	B
2 ₅₉ ^h	H	H	OCF ₃	H	H	Cl	H	7.62	> 300	A

(continued on next page)

Table 1 (continued)

Compound	R ₆	R ₇	R ₈	R ₉	R _{6'} (2')	R _{5'}	R _{4'}	pIC ₅₀ ^a	MP (°C) ^b	Cryst. solvent ^c
2 ₆₀ ^h	H	H	OCF ₃	H	H	F	H	9.40	> 300	A
2 ₆₁ ^h	H	H	OCF ₃	H	H	NO ₂	H	7.20	> 300	D
2 ₆₂ ^h	H	H	OCF ₃	H	H	NH ₂	H	9.62	> 300	B
2 ₆₃ ^h	H	H	OCF ₃	H	H	H	Br	7.82	> 300	B
2 ₆₄ ^h	H	H	OCF ₃	H	H	H	CH ₃	8.79	> 300	A
2 ₆₅ ^h	H	H	OCF ₃	H	H	H	Cl	7.90	> 300	A
2 ₆₆ ^h	H	H	OCF ₃	H	H	H	F	9.00	> 300	A
2 ₆₇ ^h	H	H	OCF ₃	H	H	H	NO ₂	7.40	> 300	C
2 ₆₈ ^h	H	H	OCF ₃	H	H	H	NH ₂	9.10	> 300	B
2 ₆₉ ^h	H	H	OCF ₃	H	H	H	OCH ₃	9.22	> 300	B
2 ₇₀ ^h	H	H	OCF ₃	H	H	H	OH	9.63	284–287	A
2 ₇₁	H	H	OCF ₃	H	H	H	N(CH ₃) ₂	8.26	285 (dec)	B
2 ₇₂	H	H	OCF ₃	H	H	H	COOH	5.50	> 300	A
2 ₇₃	H	H	OCF ₃	H	H	NH ₂	OH	7.98	> 300	G
2 ₇₄	H	H	OCF ₃	H		2-Pyrid-2'-yl		10.35	> 300	A
2 ₇₅	H	H	OCF ₃	H		2-Pyrimid-2'-yl		8.50	> 300	A
2 ₇₆ ^f	H	H	H	OH	H	H	H	9.62	—	—
2 ₇₇	H	H	H	OH	H	NH ₂	H	8.82	> 300	A
2 ₇₈ ^f	H	H	H	OCH ₃	H	H	H	8.84	—	—
2 ₇₉	H	H	H	OCH ₃	H	NH ₂	H	8.85	265–269	G
2 ₈₀	H	H	H	OCH ₃	H	NO ₂	H	8.45	300	D
2 ₈₁	H	H	H	OCH ₃	H	H	OH	8.67	> 300	A
2 ₈₂	H	H	H	OCH ₃	H	H	OCH ₃	8.94	> 300	B
2 ₈₃ ^k	F	H	F	H	H	H	H	7.87	—	—
2 ₈₄ ^k	F	H	F	H	H	F	H	8.02	—	—
2 ₈₅ ^k	F	H	F	H	H	H	Br	6.79	—	—
2 ₈₆ ^k	F	H	F	H	H	H	OCH ₃	8.12	—	—
2 ₈₇ ^h	F	H	F	H		2-Pyrid-2'-yl		7.82	> 300	A
2 ₈₈ ^h	F	H	F	H		2-Pyrimid-2'-yl		6.47	> 300	A
2 ₈₉ ^h	F	H	F	H		2-Pyrazin-2'-yl		6.94	> 300	A
2 ₉₀ ^k	H	Cl	H	Cl	H	H	H	8.43	—	—
2 ₉₁ ^h	F	F	F	H	H	H	H	7.70	> 300	A
2 ₉₂ ^h	F	F	F	H	H	H	CH ₃	7.15	> 300	A
2 ₉₃ ^h	F	F	F	H	H	H	Cl	7.13	> 300	A
2 ₉₄ ^h	F	F	F	H	H	H	F	7.68	> 300	A
2 ₉₅ ^h	F	F	F	H	H	H	OCH ₃	8.14	> 300	A
2 ₉₆ ^h	H	OCH ₃	OCH ₃	OCH ₃	H	H	H	8.90	298–301	A
2 ₉₇ ^h	H	OCH ₃	OCH ₃	OCH ₃	H	H	COOH	5.52	> 300	D
2 ₉₈ ^h	H	OCH ₃	OCH ₃	OCH ₃		2-Pyrid-2'-yl		8.50	> 300	A
2 ₉₉ ^h	H	OCH ₃	OCH ₃	OCH ₃		2-Pyrimid-2'-yl		7.24	297 (dec)	A
2 ₁₀₀ ^h	H	OCH ₃	OCH ₃	OCH ₃		2-Pyrazin-2'-yl		8.94	297 (dec)	A
2 ₁₀₁	6,7-BENZOFUSED		H	H	H	H	H	6.00	> 300	E
2 ₁₀₂	H	H	8,9-BENZOFUSED		H	H	H	8.14	> 300	B
2 ₁₀₃ ⁱ	H	7,8-OCH ₂ O		H	H	H	H	8.52	—	—
2 ₁₀₄ ⁱ	H	7,8-OCH ₂ O		H	H	H	OCH ₃	8.14	—	—
2 ₁₀₅	H	H	OC ₄ H ₉	H	H	H	H	8.54	237–40	B
2 ₁₀₆	H	H	OC ₄ H ₉	H	F	H	H	9.08	240–243	A
2 ₁₀₇	H	H	OC ₄ H ₉	H	H	H	Cl	7.45	> 300	A

^aBinding data from the displacement of [³H]flunitrazepam, ref 32.^bReported only for the newly synthesised compounds and for compounds already described but lacking those data.^cCrystallization solvent(s): A: EtOH; B: EtOH + H₂O; C: DMF; D: DMF + H₂O; E: MeOH; F: AcOEt; G: purified by column chromatography (dichloromethane:methanol, 18:2).^dRef 29.^eRef 23, pIC₅₀s of compounds **2**₂ and **2**₉ have been redetermined. Compounds **2**₂, **2**₉ and **2**₁₀ are better known as CGS-8216, CGS-9896 and CGS-9895, respectively.^fRef. 22, pIC₅₀ of compound **2**₁₇ has been redetermined.^gN₅-Methyl derivatives.^hMolecules from our previous paper (ref 18).ⁱRef 28.^jRef 26.^kRef 21.^lRef 30.^mRef 31, pIC₅₀ of compounds **2**₁₈ and **2**₂₀ have been redetermined.ⁿRef 33, pIC₅₀ has been redetermined.

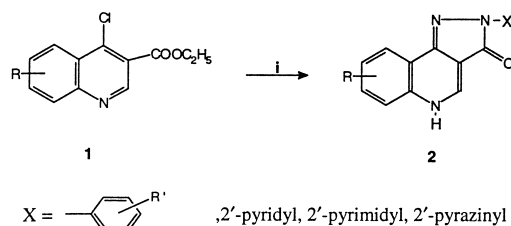
The pIC₅₀ values reported in Table 1 have been normalized using CGS-8216 (**2**₂) and CGS-9896 (**2**₉) as internal reference compounds. Literature data in Table 1 were also normalized by the same method.

Quantitative structure–activity relationship (QSAR) studies

An extensive review on the quantitative structure–activity relationships of several classes of central ben-

Table 2. ^1H NMR and IR spectral data of some representative PQs (2)

Compound	^1H NMR (δ , ppm; J = Hz)	IR (cm^{-1})
2 ₅	(DMSO- d_6) 7.50–7.74 (m, 4H), 7.97 (dd, 1H), 8.22 (d, 1H), 8.63 (dd, 1H), 8.75 (s, 1H, H-4), 9.08 (n t, 1H, H-2'), 12.88 (br s, 1H, NH, D ₂ O exchangeable).	1618 (CO)
2 ₂₁	(DMSO- d_6) 7.17 (t, 1H), 7.42 (t, 2H, H-(3',5')), 8.13 (d, 2H, $J_{\text{orto}} = 8.2$ Hz), 8.20 (dd, 1H, H-8, $J_{8-9} = 8.8$, $J_{8-6} = 2.0$ Hz), 8.32 (d, 1H, H-9, $J_{9-8} = 8.8$ Hz), 8.44 (n d, 1H, H-6, $J_{6-8} = 2.0$ Hz), 8.81 (s, 1H, H-4), 12.94 (br s, 1H, NH, D ₂ O exchangeable).	1620 (CO)
2 ₂₃	(DMSO- d_6) 7.10 (dd, 1H, H-8, $J_{8-9} = 1.8$), 7.20 (d, 1H, H-6, $J_{6-8} = 8.7$, $J_{8-6} = 1.8$ Hz), 7.23 (d, 1H, PhH), 7.50 (t, 2H, PhH), 8.12 (d, 1H, H-9, $J_{9-8} = 8.7$ Hz), 8.3 (d, 2H, PhH), 8.65 (s, 1H, H-4), 10.44 (br s, 1H, OH, D ₂ O exchangeable).	1616 (CO)
2 ₃₃	(DMSO- d_6) 3.88 (s, 3H, OCH ₃), 7.24–7.36 (m, 2H, H-7 and H-5 pyrimidinyl), 7.51 (d, 1H, H-9, $J_{9-7} = 2.6$ Hz), 7.63 (d, 1H, H-6, $J_{6-7} = 9.2$ Hz), 8.61 (s, 1H, H-4), 8.82 (d, 2H, H-(4, 6) pyrimidinyl), 12.65 (br s, 1H, NH, D ₂ O exchangeable).	1647 (CO)
2 ₃₅	(DMSO- d_6) 1.39 (t, 3H, CH ₃ -CH ₂ O), 4.18 (q, 2H, CH ₃ -CH ₂ O), 7.28 (dd, 1H, H-7, $J_{7-6} = 9.0$, $J_{7-9} = 2.4$ Hz), 7.48 (d, 2H, PhH, $J_{\text{orto}} = 8.8$ Hz), 7.55 (d, 1H, H-9, $J_{9-7} = 2.4$ Hz), 7.66 (d, 1H, H-6, $J_{6-7} = 9.0$ Hz), 8.29 (d, 2H, PhH, $J_{\text{orto}} = 8.8$ Hz), 8.65 (s, 1H, H-4), 12.82 (br s, 1H, NH, D ₂ O exchangeable).	1618 (CO)
2 ₄₂	(DMSO- d_6) 0.89 (t, 3H, CH ₃ -CH ₂ -CH ₂ -CH ₂ -), 1.31 (st, 2H, CH ₃ -CH ₂ -CH ₂ -CH ₂ -), 1.61 (qt, 2H, CH ₃ -CH ₂ -CH ₂ -CH ₂ -), 2.73 (t, 2H, CH ₃ -CH ₂ -CH ₂ -CH ₂ -), 3.83 (s, 3H, OCH ₃), 7.51 (dd, 1H, H-7, $J_{7-6} = 8.4$, $J_{7-9} = 1.3$ Hz), 7.61 (d, 1H, H-6, $J_{6-7} = 8.4$ Hz), 8.01 (d, 3H, H-9 and 2PhH), 8.39 (d, 1H, H-4, $J_{\text{orto}} = 8.7$ Hz), 8.70 (s, 1H, H-4), 12.82 (br s, 1H, NH, D ₂ O exchangeable).	1667 (CO)
2 ₇₄	(DMSO- d_6) 7.29 (td, 1H, H-5 pyridyl), 7.72 (dd, 1H, H-7, $J_{7-6} = 9.1$, $J_{7-9} = 2.0$ Hz), 7.85–7.99 (m, 2H, H-6 and 1H pyridyl), 8.07 (u d, 1H, H-9), 8.25 (d, 1H, H-3 pyridyl, $J_{3-4} = 8.1$ Hz), 8.55 (dd, 1H, H-6 pyridyl), 8.83 (s, 1H, H-4), 12.99 (br s, 1H, NH, D ₂ O exchangeable).	1665 (CO)
2 ₇₇	(DMSO- d_6) 5.21 (br s, 2H, NH ₂ , D ₂ O exchangeable), 6.41 (d, 1H), 6.98 (d, 1H), 7.07 (t, 1H, H-7), 7.20 (d, 1H), 7.33–7.40 (m, 2H), 7.52 (t, 1H, H-2'), 8.72 (s, 1H, H-4), 9.58 (s, 1H, OH, D ₂ O exchangeable), 12.86 (br s, 1H, NH, D ₂ O exchangeable).	1624 (CO)
2 ₈₁	(DMSO- d_6) 4.05 (s, 3H, OCH ₃), 6.90 (d, 2H, PhH, $J_{\text{orto}} = 8.8$ Hz), 7.14 and 7.31 (u dd, 2H, H-(6,8), 7.62 (t, 1H, H-7), 8.02 (d, 2H, PhH, $J_{\text{orto}} = 8.8$ Hz), 8.63 (d, 1H, H-4, $J_{\text{CH-NH}} = 5.7$ Hz), 9.40 (s, 1H, OH, D ₂ O exchangeable), 12.61 (d, 1H, NH, $J_{\text{NH-CH}} = 5.7$ Hz, D ₂ O exchangeable).	1639 (CO)
2 ₁₀₁	(DMSO- d_6) 7.22 (t, 1H, H-4'), 7.50 (t, 2H, H-(3', 5')), 7.75–7.89 (m, 2H), 8.06–8.31 (m, 5H), 8.70 (s, 1H, H-4), 8.78 (u dd, 1H, H-6), 13.01 (br s, 1H, NH, D ₂ O exchangeable).	1636 (CO)
2 ₁₀₂	(DMSO- d_6) 7.25 (t, 1H, H-4'), 7.54 (t, 2H, H-(3', 5')), 7.72–7.98 (m, 3H), 8.14–8.26 (m, 3H), 8.39 (d, 1H, H-7, $J_{7-6} = 8.4$ Hz), 8.89 (s, 1H, H-4), 9.93 (d, 1H, H-6, $J_{6-7} = 8.4$ Hz), 13.17 (br s, 1H, NH, D ₂ O exchangeable).	1636 (CO)
2 ₁₀₆	(DMSO- d_6) 0.93 (t, 3H, CH ₃ -CH ₂ -CH ₂ -CH ₂ O), 1.44 (st, 2H, CH ₃ -CH ₂ -CH ₂ -CH ₂ O), 1.74 (qt, 2H, CH ₃ -CH ₂ -CH ₂ -CH ₂ O), 4.08 (t, 2H, CH ₃ -CH ₂ -CH ₂ -CH ₂ O), 7.24 (d, 1H, $J_{\text{meta}} = 2.7$ Hz), 7.28–7.42 (m, 3H), 7.47 (d, 1H, H-9, $J_{9-7} = 2.7$ Hz), 7.57 (dd, 1H), 7.65 (d, 1H, H-6, $J_{6-7} = 8.9$ Hz), 8.66 (s, 1H, H-4), 12.80 (br s, 1H, NH, D ₂ O exchangeable).	1654 (CO)

**Scheme 1.** R and R' as reported in Table 1 (i) R'-phenylhydrazine (ethanol reflux); α -(N)-heterocyclhydrazines (rt).

zodiazepine receptor (CBR) ligands, not inclusive of PQ compounds, has been reported by Hansch.³⁵ Subsequently, a limited number of PQs has been subjected to a QSAR analysis leading to some interesting results, preliminarily reported by us in this journal.¹⁸

In order to gain further indications at a quantitative level on the topography of the BzR binding sites, a QSAR study of a larger series of PQs, including all the compounds reported in our previous paper,¹⁸ was carried out by the classical Hansch approach.³⁶ Unfortunately, the lack of parameters for some substituents and the presence of several polysubstituted congeners, quite difficult to be correctly parameterised, prevented a safe application of the classical QSAR approach to the overall data set. The Hansch approach, on the other hand, is well suited for congeneric series and for this reason the QSAR analysis was conducted separately on the 6-, 7-, and 8-substituted 2-aryl congeners and on *meta* and *para* substituted 2-phenyl congeners of the 8-OCF₃ derivative 2₅₃.

The multiple linear regression analysis (MLR) with cross-validation was performed on the binding data in Table 1 using the chemical descriptors listed in Table 4.

The electronic and hydrophobic effects of substituents were assessed by the Hammett (σ) and Hansch (π) substituent constants, whereas the molar refractivity (MR), the van der Waals volume (vW) and the STERIMOL Verloop parameters (L , B_1 and B_5) were employed to model bulkiness and polarizability effects.³⁷

The following equations were derived for the indicated subsets:

- 8 substituted, 2 phenyl congeners

$$\text{pIC}_{50} = -0.312(\pm 0.04)vW + 9.662(\pm 0.11)$$

$$n = 11, r^2 = 0.879, s = 0.211, Q^2 = 0.781, F = 65.14 \quad (1)$$

- 7 substituted, 2-phenyl congeners

$$\text{pIC}_{50} = -1.066(\pm 0.32)vW + 9.372(\pm 0.30)$$

$$n = 8, r^2 = 0.618, s = 0.412, Q^2 = 0.292, F = 9.69 \quad (2)$$

- 6-substituted, 2-phenyl congeners

$$\begin{aligned} \text{pIC}_{50} &= -2.613(\pm 0.47)\text{vW} + 9.347(\pm 0.45) \\ n &= 5, r^2 = 0.912, s = 0.543, Q^2 = 0.801, \\ F &= 31.23 \end{aligned} \quad (3)$$

- 8-OCF₃, 2-phenyl *meta* and *para* substituted congeners

$$\begin{aligned} \text{pIC}_{50} &= -1.343(\pm 0.32)\sigma_m, p - 0.960(\pm 0.30)\text{vW}_{m, p} \\ &\quad + 9.479(\pm 0.28) \\ n &= 15, r^2 = 0.774, s = 0.448, \\ Q^2 &= 0.723, F = 20.50 \end{aligned} \quad (4)$$

In eqs. (1)–(4), *n* is the number of compounds, *r*² is the squared correlation coefficient, *s* is the standard deviation, *Q*² is the squared crossvalidation coefficient and *F* is the Fisher ratio. The standard errors of the regression coefficients are reported in parentheses. Eqs. (1), (3), and (4) present acceptably good statistics in terms of fitting power, whereas eq. (2) gave poorer statistics, especially in terms of predictive capacity. Eqs. (1), (2), and (3) point out a significant steric hindrance at 8-, 7-, and 6-positions, respectively, as accounted for by the substituent van der Waals volume *vW*. The negative coefficient with *vW* is much higher in eq. (3) than in eqs. (1) and (2) and this suggests a stronger steric effect at position 6, which may hamper the formation of a hydrogen bond of the N₅-H group, as hypothesised in several pharmacophore models.³⁸

The negative sign of σ and *vW* in eq. (4) indicates that the binding of the 2-phenyl-substituted ring at the L₁ (L₂) receptor regions (see pharmacophore model in Fig. 1) is favoured by small electron donor substituents at both *meta* and *para* positions. An equation of comparable statistical value can be obtained by substituting *vW* with MR. Compounds **2**₇₂, bearing at *para* position a carboxylic group, resulted in a strong outlier and was excluded from the regression. The drop of **2**₇₂ may be justified considering that the carboxylic group is ionised at physiological pH, and that the carboxylate anion has less accurately defined electronic and steric parameters. Moreover, it would be the only charged compound of this set of ligands likely constituting a possible leverage point, all the other data being referred to uncharged ligands. The lipophilic character of the substituents seems to play a marginal role in the receptor–ligand interaction and this casts some doubt about the lipophilic nature assigned in several pharmacophore models to some receptor regions, especially the one named L₂, which is close to the *para* position of the 2-phenyl ring (Fig. 1).

In addition, eq. (4) illustrates a limited steric accessibility at the L₂ region, as also noticed in a previous study,¹⁶ and suggests that a π – π stacking interaction,⁴⁰ in which the substituted phenyl ring acts as π electron donor, might take place at the L₁ receptor region.

Eqs. (1)–(4) can be more efficiently interpreted by the pictorial QSAR reported in Figure 2.

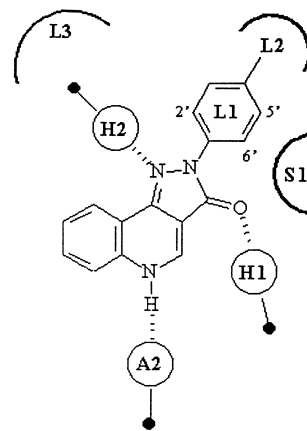


Figure 1. Proposed pharmacophore model¹³ for BzR. The main binding sites for pyrazoloquinoline CGS-8216 (**2**₂) are indicated as H₁ and H₂ (HB donor sites), A₂ (HB acceptor site), L₁ and L₂ (hydrophobic sites). L₃ is another lipophilic region reached by the 5-phenyl ring of classical benzodiazepine. S₁ represents a sterically inaccessible region. Binding to H₂ and A₂ is not necessary for inverse agonist activity.³⁹

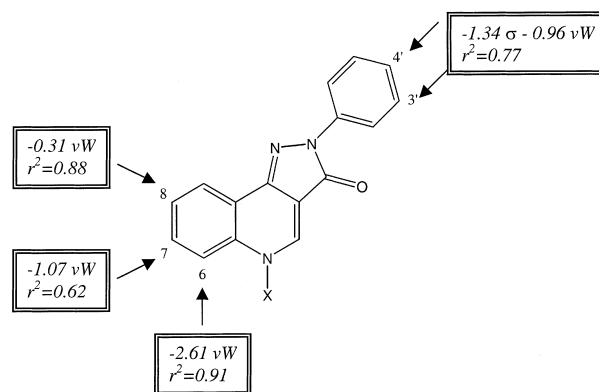


Figure 2. Pictorial QSAR of PQs showing regression and squared correlation coefficients of the descriptors in each positional QSAR.

From the previous Hansch equations based on the substituent effects on single positions, a comprehensive regression equation was derived to describe the *pIC*₅₀ changes by considering at once all the relevant effects already seen, singularly, at positions 6, 7, 8, 3' (*meta*) and 4' (*para*), and parameterised now by *vW*₆, *vW*₇, *vW*₈, $\sigma_{m,p}$ and *vW*_{m,p}, respectively.

The following comprehensive equation was formulated:

- 6,7,8-monosubstituted-2-phenyl congeners and 8-OCF₃ 2-phenyl, substituted congeners:

$$\begin{aligned} \text{pIC}_{50} &= -2.999(\pm 0.26)\text{vW}_6 - 1.251(\pm 0.24)\text{vW}_7 \\ &\quad - 0.268(\pm 0.07)\text{vW}_8 - 1.405(\pm 0.30)\sigma_{m, p} \\ &\quad - 0.683(\pm 0.17)\text{vW}_{m, p} + 9.955(\pm 0.20) \\ n &= 36, r^2 = 0.849, s = 0.421, Q^2 = 0.750, \\ F &= 33.89 \end{aligned} \quad (5)$$

Also in the derivation of eq. (5), compounds **2**₇₂ was omitted.

Eq. (5) gives a straightforward overall picture of the main physicochemical interactions, underlying the BzR binding of PQs and, as expected, it fits well with the pictorial QSAR in Figure 2. On the basis of these results, two new compounds, namely compounds **2**₇₁ and **2**₇₃, were designed, synthesised and tested by taking into account, in particular, the favourable effects on the binding affinity exerted by electron donor groups (negative σ values) in positions *meta* and *para*.

Indeed, we obtained two very active compounds whose binding affinity was acceptably well predicted by eq. (4): **2**₇₁ ($\text{pIC}_{50(\text{obs})} = 8.53$, $\text{pIC}_{50(\text{pred.})} = 8.42$) and **2**₇₃ ($\text{pIC}_{50(\text{obs})} = 8.70$, $\text{pIC}_{50(\text{pred.})} = 9.07$).

3-D QSAR study: comparative molecular field analysis

Since the valuable indications coming from the preceding 2-D QSAR study refer to a relatively small number of congeneric ligands (36) we decided to extend our investigations to the whole set of ligands (106 compounds) by using a 3-D QSAR approach, that is the Comparative Molecular Field Analysis (CoMFA⁴¹).

CoMFA is a widely used tool for studying quantitative structure–activity (property) relationships (QSAR, QSPR) at the three-dimensional level.⁴² Unlike the traditional Hansch analysis, which makes use of substituent parameters, CoMFA relates the biological activity (target property) of a series of molecules with their steric and electrostatic fields sampled at grid points defining a large 3-D box around the molecule. CoMFA descriptors are commonly constituted by steric (Lennard-Jones) and electrostatic (Coulomb) potentials computed for each molecule, at each grid point, by means of a suitable probe, usually an *sp*³ carbon atom with a charge of +1. Partial Least Squares (PLS⁴³) is used as the regression method to find the relations between independent variables (steric and electrostatic potentials) and biological activity (dependent variable). PLS analysis produces model equations which explain the variance in the target property in terms of the independent variables.⁴⁴ The optimum number of components (latent variables) is determined by cross-validation and the model predictive ability is assessed by cross-validated correlation coefficient (r_{cv}^2 , Q^2).⁴⁵ The graphical representation of CoMFA results as isocontour maps indicated the regions where the variation in steric and electrostatic properties of different molecules in a data set is correlated with the variation of biological activity.

Classical CoMFA studies rely on standard steric and electrostatic molecular fields to model receptor–ligand interactions. Unfortunately, as demonstrated in several investigations,⁴⁶ these two fields are not always able to appropriately describe all binding forces. Furthermore, CoMFA describes only the enthalpic component of the ligand–receptor interactions. Introducing the molecular lipophilicity potential (MLP⁴⁷) as an additional field has been shown to significantly improve the descriptive, interpretative and predictive power of CoMFA in many cases.⁴⁸ The MLP encodes indeed hydrogen bonds and hydrophobic interactions not sufficiently described by

the steric and electrostatic fields and also includes an entropy component.⁴⁹ For these reasons, the CoMFA methodology, with the inclusion of the MLP, was selected as the more appropriate tool to study the SARs of our CBR ligands.

Molecular models were constructed from the fragment library of SYBYL 6.6 and their geometry optimised by the AM1 Hamiltonian within the suite of program MOPAC.⁵⁰ Each ligand molecule was subjected to a conformational analysis, when necessary, through a systematic search and the minimum energy conformers were selected for the superposition.

The molecular alignment is the most critical step in a CoMFA study.⁵¹ In the present work, dealing with congeneric compounds, the molecular overlay was performed by choosing as the anchor moiety the common pyrazolo-quinoline ring. With few exceptions, the substituents in the quinoline ring were used in their minimum energy conformations. The relative orientation of the phenyl and azaheterocyclic rings in position 2, as well as the diverse topology of the *ortho* and *meta* substituents, were analysed in full detail.

For the sake of clarity and a more prompt comparison, the binding affinities of selected 8-substituted ligands bearing phenyl, *ortho*-fluorophenyl and nitrogen heterocyclic substituents at 2 position were taken from Table 1 and collected in Table 3. The analysis of data in Table 3 reveals that the introduction of a fluorine atom in *ortho* position, as well as the replacement of the phenyl ring with a 2-pyrid-2'-yl ring, always yielded higher affinities, the strongest effect being seen for **2**₇₄. A less definite effect was observed for the 2-pyrimidin-2'-yl and 2-pyrazin-2'-yl substituted ligands.

It was interesting to note that the pyridyl nitrogen and the fluoro atom in *ortho* position can occupy close regions and that, when facing the pyrazole N₁, a likely three-centred HB could be formed. Strong steric and repulsive electrostatic interactions could prevent the formation of a similar HB with larger sized *ortho*-substituents. In principle, a similar three-centred HB could also be formed with the oxygen of the 3-carbonyl group, in place of the N₁ pyrazole nitrogen, with the phenyl

Table 3. Chemical structures and binding affinity of selected 2,8-di-substituted PQs **2**

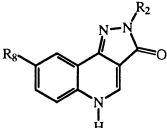
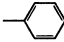
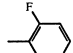
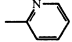
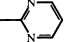
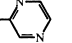
					
R ₂ /R ₈					
<i>n</i> -C ₄ H ₉	9.00 (2 ₃₉)	9.18 (2 ₄₀)	9.50 (2 ₄₃)	8.77 (2 ₄₄)	9.22 (2 ₄₅)
<i>c</i> -C ₆ H ₁₁	8.35 (2 ₄₆)	—	8.60 (2 ₄₈)	8.36 (2 ₄₉)	8.16 (2 ₅₀)
OCF ₃	9.15 (2 ₅₃)	9.40 (2 ₅₄)	10.35 (2 ₇₄)	8.50 (2 ₇₅)	—
OC ₄ H ₉	8.54 (2 ₁₀₅)	9.08 (2 ₁₀₆)	—	—	—
Cl	9.37 (2 ₂₉)	—	9.39 (2 ₃₀)	—	—

Table 4. Substituent parameters used for the derivation of regression equations (1)–(5)^a

Subs.	σ_p^b	π	MR ^c	vW	L	B ₁	B ₅
H	0.00	0.00	0.10	0.08	2.06	1.00	1.00
OCF ₃	0.35	1.04	0.79	1.60	4.57	1.35	3.61
<i>n</i> -C ₄ H ₉	−0.16	2.13	1.96	3.12	6.17	1.52	4.54
<i>c</i> -C ₆ H ₁₁	−0.22	2.51	2.67	4.26	6.17	1.91	3.49
Cl	0.23 (0.37)	0.71	0.60	1.07	3.52	1.80	1.80
OCH ₃	−0.27	−0.02	0.79	1.49	3.98	1.35	3.07
OBn	−0.23	1.66	3.17	4.95	8.20 ^d	1.61 ^d	4.44 ^d
OH	−0.37	−0.67	0.28	0.49	2.74	1.35	1.93
F	0.06 (0.34)	0.14	0.09	0.36	2.65	1.35	1.35
OC ₂ H ₅	−0.24	0.38	1.25	2.42	4.80	1.35	3.36
CH ₃	−0.17 (−0.07)	0.56	0.57	1.01	2.87	1.52	2.04
CF ₃	0.54	0.88	0.50	1.11	3.30	1.99	2.61
Br	0.23 (0.39)	0.86	0.89	1.32	3.82	1.95	1.95
NO ₂	0.78 (0.71)	−0.28	0.74	1.20	3.44	1.70	2.44
NH ₂	−0.66 (−0.16)	−1.23	0.54	0.67	2.78	1.35	1.97
OC ₄ H ₉	−0.32 (0.10)	1.55	2.17	4.27	6.86	1.35	4.79

^aData taken from ref 37. See text for the significance of parameter symbols.^b σ values for *meta* substituents (σ_m) are reported in parentheses.^cScaled by 0.1.^dReferring to the benzyloxy group in a planar conformation.

ring in a different conformation. Taking into account the most widely accepted pharmacophore model of CBR ligands (see Fig. 1) this latter orientation should be less favoured because of the steric bulk at S₁. Interestingly, a three-centred hydrogen bond has been used to explain the high binding affinities observed for other BZ-receptor ligands such as certain benzodiazepines and β -carbolines, which are thought to interact with the same HB donor site (H₁).⁵²

Also the 2-pyrimidin-2'-yl and 2-pyrazin-2'-yl substituted ligands might form, in principle, a three-centred HB analogously to the 2-pyrid-2'-yl congeners and therefore a higher affinity could be expected. Data in Table 3 show that this is not the case; most likely the presence of a second heterocyclic nitrogen might generate additional important interactions leading to more complex structure–affinity relationships.

In order to furnish a significant support to the hypothesis of a three-centred HB formation, a quantum mechanical study was undertaken on selected PQs ligands, namely the 8-OCF₃ derivatives **2**₅₃, **2**₅₄, **2**₇₄ and **2**₇₅ (Table 3). It should be anticipated that three-centred HBs have been studied, both theoretically and experimentally, only when nitrogen and oxygen atoms are involved.⁵³ In contrast, no investigation has been made yet on a three-centred HB involving a fluorine atom. Indeed, for the F-C group, the so called ‘organic fluorine’, even the formation of a simple HB of OH-FC and NH-FC type has been the object of a strong dispute in the scientific chemical community and only very recently has it been proved and accepted.^{54–56}

Our theoretical study was carried out by means of MIPSIM, a useful tool for the analysis and comparison of Molecular Interaction Potentials (MIPs). MIPSIM⁵⁷ is an evolution of the MEPSIM^{58,59} program that allows the calculation of the potentials to be analysed and compared, as the interaction energies between a molecule and proper probes, computed in each node of a grid all

around it. In our case, the proton atom was chosen as the probe and therefore our calculated MIPs are indeed classical Molecular Electrostatic Potentials (MEPs).

To compute and locate the MEP minima, the *ab initio* program GAMESS⁶⁰ was used within the MIN module of MIPSIM. The MIN calculation was performed on a 40×33×19 Å cubic grid lattice (default spacing=0.5 Å) giving a total number of points equal to 25,080. The conjugate gradient algorithm was selected as the optimisation method and all the energy minima under a value of 5 kcal/mol were optimised with a tolerance of the gradient=0.01 kcal/mol Å. The charges of the ligands were calculated using the RHF/6-31G basis set implemented in the GAMESS package.

The results of our study are reported in Figure 3, where the main minima, expressed in kcal/mol and indicated by violet balls, are represented only for the moiety of interest, that is the 2-substituted 3-pyrazolone moiety.

Interestingly, Figure 3 shows only three main minima for each moiety, two close to the two carbonyl lone pairs and the third located between the N₁ and the N'₁ heterocyclic nitrogens or the N₁ and the *ortho*-fluoro atom.

The minima near the carbonyl groups, whose intensities are comparable for all the analysed compounds, are positioned in a symmetric way with respect to the carbonyl oxygen atom, with the notable exception of the pyrimidinyl congeners, where the “upper” minimum is close to the N'₃ nitrogen.

The existence of only one minimum between N₁ and N'₁ (or *ortho*-fluoro) atoms may support the hypothesis of a formation of a three-centred HB where the hydrogen atom is very near to those minima.

Interestingly, the depth of the minima seems related to the observed binding affinities, with the exception of the pyrimidin-2'-yl derivative (**2**₇₅), that, as already anticipated,

could give rise to further interactions driven by the presence of the second heterocyclic nitrogen.

The previous analysis gave us precise indications as to the alignment of *ortho*-substituted 2-phenyl and 2-heterocyclic congeners.

As far as the alignment of the *meta* derivatives is concerned, the two possible diverse topologies were taken into account and the one giving the best statistical model was retained.

In summary, the *ortho*-fluoro substituents were placed in position 2', all the other *ortho*-substituents being in position 6'; *meta*-substituents were in position 5' and all the heterocyclic substituents were aligned with one nitrogen in position 2' (see Fig. 1 for numbering).

All the selected ligands conformations were superimposed by the RIGIDFIT option of SYBYL (poorer results always came from the FIELDFIT option) and subjected to PLS analysis in conjunction with cross-validation (CV; leave-one-out method⁶¹) to derive the optimal number of components (ONC) to be used in the subsequent analyses. The PLS run was repeated with the ONC (see below) and a number of CV groups set to zero. However, in following strictly this procedure there is a risk of obtaining overfitted models due to a relatively high number of components to be used.⁶² We therefore chose, from a plot of the squared cross-validated Q^2 versus ONC, the first maximum in the curve. The selection of a lower number of components than the ONC given by default in SYBYL yields poorer statistics in terms of r^2 and standard deviation (worse fitting), but more realistic and trustworthy models.⁶³

The statistical results of CoMFA models are represented in Table 5 and the corresponding isocontour maps are shown in Figures 4, 5, and 6. The colour code used to characterise favourable and unfavourable zones of each field is described in Table 6 and it is the same used by us and others in past studies.⁴⁸

The introduction of the MLP as third field did not improve the statistical value of the models. This was not very surprising since in the QSAR eqs. (1)–(5) derived by the classical Hansch approach no lipophilic parameters was found significant.

In a first step we derived the two-field PLS model ES1 by analysing the same data set used in the 2-D QSAR study. Model ES1 and regression eq. (5) show comparable statistics in terms of fitting power, being however the predictive ability of eq. (5) significantly better than model ES1. Interestingly, the results coming from 2-D and 3-D QSAR approaches are in quite good agreement

Table 5. Statistical results from the CoMFA study

Model	n	NOC ^a	Q ^{2b}	sd _{cv} ^c	r ^{2d}	sd ^e	Fields
ES1	36	4	0.536	0.727	0.917	0.308	Steric and Electrostatic
S2	106	6	0.404	0.838			Steric
E2	106	3	0.434	0.805			Electrostatic
ES2	106	7	0.632	0.662	0.886	0.369	Steric and Electrostatic

^aNumber of optimal components.

^bSquared cross-validation correlation coefficient.

^cStandard deviation of errors of predicted values.

^dSquared correlation coefficient.

^eStandard deviation of errors of fitted values.

Figure 3. MEP minima (kcal/mol, violet balls) on the 2-substituted 3-pyrazolone moiety of (clockwise) **2**₅₃, **2**₅₄, **2**₇₄ and **2**₇₅ ligands are marked as violet balls.

Figure 4. Electrostatic and steric isocontour maps from model ES1. Electrostatic contour levels: white=0.04, magenta=−0.034. Steric contour levels: red=−0.070, green=0.044. Molecules shown to help interpretation are: **2**₁₅ (pIC₅₀=5.73), **2**₁₆ (pIC₅₀=5.66), **2**₆₁ (pIC₅₀=7.20), **2**₂₀ (pIC₅₀=7.64), **2**₃₆ (pIC₅₀=9.70), **2**₆₀ (pIC₅₀=9.40), **2**₇₀ (pIC₅₀=9.63), and **2**₂₄ (pIC₅₀=9.54).

Table 6. Colour code of CoMFA isocountour maps in Figures 3, 4, and 5

Field or field component	Increased affinity	Decreased affinity
Steric field	Green	Red
Electrostatic field (positive charge)	White	Magenta
Electrostatic field (negative charge)	Magenta	White

interesting to note that to the electronic effects accounted for by σ in eqs (4) and (5), correspond to two favourable electrostatic signals, coloured in magenta in Figure 4, close to positions 5' and 4' of the 2-phenyl ring. They may be ascribed to electron-rich groups in those positions of the 2-phenyl ring.

In a second step the CoMFA study was extended to the whole set of PQ ligands. The four 4'-COOH derivatives (**2**₄₁, **2**₄₇, **2**₇₂ and **2**₉₇) were considered in their ionised form in the derivation of the two-field PLS model ES2, which presents satisfactory statistics in terms of both fitting and predictive power and agrees well with the 2-D QSAR models derived by MLR. At physiological (binding) pH these acidic ligands should indeed be completely ionised. However, their elimination from the model, as well as their inclusion as unionised species, led to poorer PLS models (results not shown).

The isocontour maps were therefore developed from PLS model ES2. In the steric map of Figure 5, sterically allowed regions (green polyedra) can be seen close to 5', 8 and, to a lesser extent, 2' positions. Strong unfavourable steric interactions, indicated by red polyedra, can be localised near positions 5 and 6 of the quinoline ring and position 4' of the 2-phenyl ring. Additional detrimental steric interactions can be located at positions 7 and 8. Most of these signals (see also Fig. 4) are easily interpretable considering the strong drop of affinity observed for N-5 substituted (compound **2**₁₁), 6-substituted (compound **2**₁₅), 7-substituted (compound **2**₂₀) and 8-substituted (compound **2**₄₂) ligands. The strong negative steric signal at position 4' may be due to very low activity ligands such as the acidic compounds **2**₄₁, **2**₄₇, **2**₇₂ and **2**₉₇, and the ester **2**₄₂, the latter being shown on the map. The electrostatic signals indicated mainly unfavourable interactions (white polyedra) for electron-rich moieties located at 6', 5', and 4' positions of the 2-phenyl ring (compounds **2**₅₅, **2**₆₁ and **2**₇₂ in Fig. 6) and at 6 and 7 positions of the quinoline moiety (compounds **2**₁₀₁ and **2**₁₅ in Fig. 6). The magenta polyedra, whose occupation by electron-rich groups increases the binding affinity, are near positions 9 (1), 4' and 1' (2'). Interestingly, an informative magenta polyhedron is placed just between positions 1 and 9, where the formation of a three-centred HB involving the N1 nitrogen and small electron donor group like the OH at position 9 in compounds **2**₇₆ and **2**₇₇ may be responsible for the observed high affinity. The synthesis and testing of derivatives bearing small sized HB accepting substituents at position 9 might prove the validity of such a hypothesis.

The favourable effects on the binding affinity caused by the replacement of the phenyl ring in position 2 with a

Figure 5. Steric isocontour maps from model ES2; contour levels: green = 0.035, red = -0.053. Molecules shown to help interpretation are: **2**₁₁ (pIC₅₀ = 6.84), **2**₁₅ (pIC₅₀ = 5.73), **2**₂₀ (pIC₅₀ = 7.64), **2**₄₂ (pIC₅₀ = 6.86), and **2**₅₈ (pIC₅₀ = 8.20).

Figure 6. Electrostatic isocontour maps from model ES2; contour levels: white = 0.05, magenta = -0.025. Molecules shown to help interpretation are: **2**₁₅ (pIC₅₀ = 5.73), **2**₅₅ (pIC₅₀ = 8.60), **2**₆₁ (pIC₅₀ = 7.20), **2**₇₂ (pIC₅₀ = 5.50), **2**₇₆ (pIC₅₀ = 9.62), and **2**₁₀₁ (pIC₅₀ = 6.00).

suggesting similar receptor–ligand interactions, as can be seen by a simple visual comparison of the negative steric signals (red polyhedra) of the contour map in Figure 4 with the pictorial QSAR in Figure 2. In the case of the electrostatic fields, no straightforward comparison can be made with the 2-D QSAR map, since, by definition, electrostatic field indicates local electronic effects, whereas classical electronic substituent parameters, like the Hammett σ used in the Hansch analysis, measure an effect on a formally distant “reaction centre”. Nevertheless, it is

pyridine ring (compare **2**₃₉ versus **2**₄₃ and **2**₄₆ versus **2**₄₈), although not completely highlighted by the isocontour maps in Figure 6, prompt us to design, synthesise and test a new potent ligand, namely compound **2**₇₄, whose binding affinity was much higher than that predicted by the ES2 model: $\text{pIC}_{50(\text{obs})} = 10.35$, $\text{pIC}_{50(\text{pred})} = 8.80$.

Conclusion and perspectives

Taken together, the results from our QSAR studies gave us coherent insights about the nature and spatial location of the main interactions underlying the binding of potent ligands at the CBR. As observed in the past in several SAR studies, the coordinated application of 2-D and 3-D QSAR methods furnishes significant insights which may complement each other in a synergic manner yielding at the 3-D molecular level a clear picture of the main forces modulating important chemical^{64,65} and biological processes.^{66–70} Our results confirm that for strictly congeneric series the traditional QSAR approach (Hansch analysis) still yields more valuable and physicochemically better interpretable models than 3-D QSAR methods.⁷¹ However, 3-D QSAR approaches⁴² play a decisive and indispensable role when structurally diverse compounds have to be examined.

Our findings are in good accordance with previous SAR studies on CBR ligands and may be used to complement existing pharmacophore models and to guide future structural modifications. Being based on a rather large array of PQ ligands, properly modified to find out significant substituent effects in the diverse positions of the quinoline and 2-phenyl rings of the lead compound CGS-8216, our results appear quite robust and reliable.

Finally, several ligands with a binding affinity significantly higher than the lead compound CGS-8216, such as compounds **2**₄, **2**₃₆ and **2**₇₆, were identified. They might constitute new chemical tools to probe CBR ligand binding site(s) and are presently being used to study in more detail structure–activity and structure–efficacy relationships.

Chemical Experimental Section

Melting points were determined on a Gallenkamp capillary melting point apparatus and are uncorrected. Elemental analyses were performed on a Perkin–Elmer elemental analyser Mod. 240 and the data for C, H, and N are within $\pm 0.40\%$ of calculated values. Spectral analyses (IR and ¹H NMR) are consistent with the indicated chemical structures. IR spectra were determined in Nujol mulls on a Perkin–Elmer 398 or a Perkin–Elmer FT-IR 1600 spectrophotometer. ¹H NMR spectra were recorded on an AC 200 Bruker instrument. The chemical shifts (δ) are relative to Me₄Si used as internal standard. The following abbreviations were used: s=singlet, d=doublet, t=triplet, dd=double doublet, q=quartet, qt=quintet, st=sextet, m=multiplet, u=unresolved, br=broad, n=narrow. The coupling constants *J* are in hertz. TLC on silica-gel plates (Merck, 60-F₂₅₄) was used for purity check and reaction

monitoring. Column chromatography on silica-gel (Merck, 70–230 mesh and 230–400 mesh ASTH for flash chromatography) was applied, when necessary, to isolate and purify the different reaction products. The unknown ethyl 4-chloroquinoline-3-carboxylates (**1a** and **1b**) are also described in this section. Physicochemical properties of the newly synthesised PQs are summarised in Table 1.

3-Carbethoxy-4-chlorobenzo(h)quinoline (1a). A mixture of 3-carbethoxy-4-hydroxybenzo(h)quinoline (10 g, 71 mmol) and phosphorus oxychloride (25 mL) was heated in a sand bath at 135 °C for 45 min. After cooling the mixture was poured on ice water and made basic with sodium carbonate. The resulting precipitate, filtered off and purified by recrystallisation from ethanol, gave a white solid, mp 115–117 °C. ¹H NMR (CDCl₃) δ 1.52 (t, 3H, CH₃-CH₂O), 4.52 (q, 2H, CH₃-CH₂O), 7.75–7.79 and 7.92–7.97 (2 m, 4H), 8.26 (d, 1H, *J*_{ortho} = 9.5 Hz), 9.28–9.33 (m, 2H). Anal. calcd for C₁₆H₁₂ClNO₂: C, 67.26; H, 4.23; N, 4.90. Found: C, 67.56; H, 4.33; N, 4.86.

3-Carbethoxy-4-chlorobenzo(f)quinoline (1b). The title compound (**1b**) was obtained following the same procedure as described above for compound **1a**; in this case the resulting crude oil was immediately used without further purification for the subsequent reaction with phenylhydrazine.

8*n*-Butyl-2-(4-carbomethoxyphenyl)pyrazolo[4,3-*c*]quinolin-3(5*H*)-one (2₄₂). The starting 8*n*-butyl-2-(4-carboxyphenyl)pyrazoloquinolinone¹⁸ (0.3 g, 0.83 mmol), added with methanol (5 mL) and concd H₂SO₄ (0.1 mL), was refluxed in an oil bath for 5–6 h. The reaction mixture was evaporated under reduced pressure, the residue was diluted with water and then washed with aqueous NaHCO₃ saturated solution. The resulting crude product was purified by recrystallisation from ethanol, mp 286 °C dec. ¹H NMR (DMSO-*d*₆) δ 0.89 (t, 3H, CH₃-CH₂-CH₂-CH₂-), 1.31 (st, 2H, CH₃-CH₂-CH₂-CH₂-), 1.61 (qt, 2H, CH₃-CH₂-CH₂-CH₂-), 2.73 (t, 2H, CH₃-CH₂-CH₂-CH₂-), 3.83 (s, 3H, OCH₃), 7.51 (dd, 1H, H-7, *J*₇₋₆ = 8.4, *J*₇₋₉ = 1.3 Hz); 7.61 (d, 1H, H-6, *J*₆₋₇ = 8.4 Hz), 8.01 (d, 3H, H-9 and 2PhH), 8.39 (d, 2H, PhH, *J*_{ortho} = 8.7 Hz), 8.70 (s, 1H, H-4), 12.82 (br s, 1H, NH, D₂O exchangeable). IR 1667 cm⁻¹ (CO). Anal. for C₂₂H₂₁N₃O₃ (C, H, N).

8-Trifluoromethoxy-2-(4-*N,N'*-dimethylaminophenyl)pyrazolo[4,3-*c*]quinolin-3(5*H*)-one (2₇₁). To a stirred solution of 8-trifluoromethoxy-2-(4-aminophenyl)pyrazolo[4,3-*c*]quinolin-3(5*H*)-one¹⁸ (576 mg, 1.6 mmol) in methanol (5 mL), containing 40% aqueous formaldehyde (0.4 mL, 5 mmol), was added a solution of sodium cyanoborohydride (105 mg, 1.6 mmol) and zinc chloride (110 mg, 0.8 mmol) in methanol (5 mL). After stirring at room temperature for 4 h, the reaction mixture was taken up in 0.1 N NaOH (10 mL), and the excess of methanol was removed under reduced pressure; the residue, purified through flash chromatography (eluent CH₂Cl₂:CH₃OH, 19:1), was recrystallised from EtOH:H₂O, mp 285 °C dec. ¹H NMR (DMSO-*d*₆) δ 2.88 (s, 6H, 2CH₃), 6.78 (d, 2H, PhH, *J*_{ortho} = 9 Hz), 7.62 (dd, 1H, H-7, *J*₇₋₈ = 8.9, *J*₇₋₉ =

1.7 Hz), 7.8 (d, 1H, H-6, J_{6-7} = 8.9 Hz), 7.9 (d, 2H, PhH, J_{ortho} = 9 Hz), 7.99 (u d, 1H, H-9), 8.68 (s, 1H, H-4), 12.8 (br s, 1H, NH, D₂O exchangeable). IR 1620 cm⁻¹ (CO). Anal. for C₁₉H₁₅F₃N₄O₅ (C, H, N).

8-Trifluoromethoxy-2-(4-hydroxy-3-nitrophenyl)pyrazolo [4,3-c]quinolin-3(5H)-one. To a stirred solution of 8-trifluoromethoxy-2-(4-hydroxyphenyl)pyrazoloquinolin-3-one¹⁸ (1.2 g, 3.3 mmol) in absolute ethanol, KNO₃ (0.34 g, 3.3 mmol), NaNO₂ (0.12 g, 1.7 mmol) as the catalyst and aqueous sulfuric acid were added. After stirring at 70 °C for 2–3 h, following the reaction course by TLC (CHCl₃:CH₃OH, 18:2, as eluent), the mixture was taken up in ice water. The resulting precipitate was filtered off and purified by chromatography on silica gel column (CHCl₃:CH₃OH, 18:2, as eluent) to afford the pure title compound, mp > 300 °C. ¹H NMR (DMSO-*d*₆) δ 7.20 (d, 1H, H-5', $J_{5'-6'}$ = 9 Hz), 7.65 (dd, 1H, H-7, J_{7-6} = 9.1 Hz), 7.80 (d, 1H, H-6, J_{6-7} = 9.1 Hz), 8.01 (d, 1H, H-9), 8.32 (dd, 1H, H-6', $J_{6'-5'}$ = 9, $J_{6'-2'}$ = 1.8 Hz), 8.72 (d, 1H, H-2', $J_{2'-6'}$ = 1.8 Hz), 8.77 (s, 1H, H-4), 10.45 (br s, 1H, OH, D₂O exchangeable), 13.02 (br s, 1H, NH, D₂O exchangeable). IR 1618 cm⁻¹ (CO). Anal. for C₁₇H₉F₃N₄O₅ (C, H, N).

8-Trifluoromethoxy-2-(3-amino-4-hydroxyphenyl)pyrazolo[4,3-c]quinolin-3(5H)-one (2₇₃). To a suspension of 8-trifluoromethoxy-2-(4-hydroxy-3-nitrophenyl) pyrazolo-[4,3-c]quinolin-3(5H)-one (160 mg, 3.9 mmol), in absolute ethanol (120 mL), 10% Pd/C (0.02 g) was added. The reaction mixture was hydrogenated at room temperature in a Parr apparatus at 40 psi for 4 h, then the catalyst was filtered off through Celite and the solution taken to dryness. The resulting residue was purified through chromatography on silica gel column (CHCl₃:CH₃OH, 18:2, as eluent) to give 2₇₃ as yellow powder, mp > 300 °C. ¹H NMR (DMSO-*d*₆) δ 4.67 (br s, 2H, NH₂, D₂O exchangeable), 6.68 (d, 1H, H-5', $J_{5'-6'}$ = 8.7 Hz), 7.20 (dd, 1H, H-6', $J_{6'-5'}$ = 8.7, $J_{6'-2'}$ = 2.3 Hz), 7.41 (d, 1H, H-2', $J_{2'-6'}$ = 2.3 Hz), 7.65 (dd, 1H, H-7, J_{7-6} = 9.2, J_{7-9} = 2.1 Hz), 7.83 (d, 1H, H-6, J_{6-7} = 9.2 Hz), 7.98 (d, 1H, H-9, J_{9-7} = 1.6 Hz), 8.70 (s, 1H, H-4), 8.95 (s, 1H, OH, D₂O exchangeable), 12.89 (br s, 1H, NH, D₂O exchangeable). IR 1618 cm⁻¹ (CO). Anal. for C₁₇H₁₁F₃N₄O₅ (C, H, N).

Biochemical Experimental Section

Chemicals

[³H]Flunitrazepam (New England Nuclear, Boston, USA) had a specific activity of 84.3 Ci/mmol and a radiochemical purity > 74.6%.

Animals

Male Sprague–Dawley rats (Charles River, Como, Italy) with body weights 150–200 g were kept under a 12 h light/dark cycle at a temperature of 23 ± 2 °C and 65% humidity. Upon arrival at the animal facilities there was a minimum of 7 days acclimatisation, during which the animals had a free access to food and water.

The animals were killed by decapitation and the brains were rapidly removed, the cerebral cortex was dissected out and was used for the measurement of [³H]flunitrazepam.

[³H]Flunitrazepam binding assay³²

Cerebral cortices were homogenised in 50 volumes of ice-cold 50 mM Tris–HCl buffer with a polytron PT 10 (setting 5, for 20 s), centrifuged at 48,000 *g* for 10 min and washed one time. The pellet was resuspended in 50 volumes of 50 mM Tris–HCl buffer (pH 7.40) and aliquots of 400 μL tissue homogenate (400–500 μg of protein) were incubated in the presence of [³H]flunitrazepam at a final concentration of 0.5 nM, in a total incubation volume of 1000 μL. The compounds were dissolved in dimethylsulfoxide and serial dilutions were made up in dimethylsulfoxide and added in 5 μL aliquots. After 60 min incubation at 4 °C, the assay was terminated by rapid filtration through glass-fibre filter strips (Whatman GF/B). The filters were rinsed with 2 × 4 mL ice-cold 50 mM Tris–HCl buffer with a cell Harvester filtration manifold (Model M-24, brandel) and transferred in plastic minivials with 3 mL scintillation fluid (AtomLight, New England Nuclear). Six to eight concentrations of the samples in triplicate were used to determine the IC₅₀ values. Non-specific binding was determined as the binding in the presence of 5 μM diazepam and was 85–90% of the total binding.

Acknowledgements

The financial support from MURST and CNR (Rome) is gratefully acknowledged. The authors wish to thank Prof. Ferran Sanz of the University Pompeu Fabra, Barcelona (Spain) for the free access to the MIPSIM software package.

References and Notes

- Kerr, I. B.; Ong, J. *J. Med. Res. Rev.* **1992**, *12*, 593.
- GABA and Benzodiazepine Receptors*; Squires, R., Ed.; CRC: Boca Raton, 1988; Vols. 1 and 2.
- Bernard, E. A. In *GABAA Receptor and Anxiety. From Neurobiology to Treatment*; Biggio, G., Sanna, E., Costa, E., Eds.; Raven: New York, 1995; pp 1–16.
- Metha, A. K.; Ticku, M. K. *Brain Res. Rev.* **1999**, *29*, 196.
- Sieghart, W. *Pharm. Rev.* **1995**, *47*, 181.
- Verdoorn, T. A.; Draguhn, A.; Ymer, S.; Seeburg, P. H.; Sakmann, B. *Neuron* **1990**, *4*, 919.
- Chang, Y.; Wang, R.; Barot, S.; Weiss, D. S. *J. Neurosci.* **1996**, *16*, 5415.
- Huang, Q.; He, X.; Ma, C.; Liu, R.; Yu, S.; Dayer, C. A.; Wenger, G. R.; McKernan, R.; Cook, J. M. *J. Med. Chem.* **2000**, *43*, 71.
- Villar, H. O.; Davies, M. F.; Loew, G. H.; Maguire, P. A. *Life Sci.* **1991**, *48*, 593.

10. Diaz-Arauzo, H.; Koehler, K. F.; Hagen, T. J.; Cook, J. M. *Life Sci.* **1991**, *49*, 207.
11. Allen, M. S.; Skolnick, P.; Cook, J. M. *J. Med. Chem.* **1992**, *35*, 368.
12. Schove, L. T.; Perez, J. J.; Loew, G. H. *Bioorg. Med. Chem.* **1994**, *2*, 1029.
13. Zhang, F.; Koehler, K. F.; Zhang, P.; Cook, J. M. *Drug Des. Dis.* **1995**, *12*, 193.
14. Harris, D. L.; Loew, G. *Bioorg. Med. Chem.*, in press.
15. Gardner, C. R. *Progr. Neuro-Psychopharmacol. Biol. Psychiatry* **1992**, *16*, 755.
16. Campagna, F.; Carotti, A.; Casini, G.; Palluotto, F.; Genchi, G.; De Sarro, G. B. *Bioorg. Med. Chem.* **1993**, *1*, 437.
17. Palluotto, F.; Carotti, A.; Casini, G.; Campagna, F.; Genchi, G.; Rizzo, M.; De Sarro, G. B. *Bioorg. Med. Chem.* **1996**, *4*, 2091.
18. Savini, L.; Massarelli, P.; Nencini, C.; Pellerano, C.; Biggio, G.; Maciocco, A.; Tuligi, G.; Carrieri, A.; Cinone, N.; Carotti, A. *Bioorg. Med. Chem.* **1998**, *6*, 389.
19. Yokoyama, N.; Ritter, B.; Neubert, A. D. *J. Med. Chem.* **1982**, *25*, 337.
20. Takada, S.; Shindo, H.; Sasatani, T.; Chomei, N.; Matsushita, A.; Masami, E.; Kawasaki, K.; Murata, S.; Takahara, Y.; Shintaku, H. *J. Med. Chem.* **1988**, *31*, 1738.
21. Shindo, H.; Takada, S.; Murata, S.; Masami, E.; Matsushita, A. *J. Med. Chem.* **1989**, *32*, 1213.
22. Wong, G.; Zi-Qiang, G.; Fryer, R. I.; Skolnick, P. *Med. Chem. Res.* **1992**, *2*, 217.
23. Fryer, R. I.; Zhang, P.; Rios, R.; Gu, Z. Q.; Basile, A. S.; Skolnick, P. *J. Med. Chem.* **1993**, *36*, 1669.
24. Schove, L. T.; Perez, J. I.; Maguire, P. A.; Loew, G. I. *Med. Chem. Res.* **1994**, *4*, 307.
25. Savini, L.; Massarelli, P.; Pellerano, C.; Fiorini, I.; Bruni, G.; Romeo, M. R. *Il Farmaco* **1993**, *48*, 65.
26. Savini, L.; Massarelli, P.; Corti, P.; Pellerano, C.; Bruni, G.; Romeo, M. R. *Il Farmaco* **1993**, *48*, 1675.
27. Trapani, G.; Franco, M.; Latrofa, A.; Carotti, A.; Genchi, G.; Serra, M.; Biggio, G.; Liso, G. *Eur. J. Med. Chem.* **1996**, *31*, 575 and references therein.
28. Ananthan, S.; Clayton, D. S.; Ealick, E. S.; Wong, G.; Evoniuk, E. G.; Skolnick, P. *J. Med. Chem.* **1993**, *36*, 479.
29. Pietrogrande, M. C.; Borea, P. A.; Biagi, G. L. *J. Chromat.* **1988**, *447*, 404.
30. Leeson L. J. (Ciba-Geigy Corp.) US 4,758,427; 19 July 1988. *Chem. Abstr.* **1989**, *110*, 199215s.
31. Yokoyama N. (Ciba-Geigy A.-G.), Eur. Pat. Appl. 22,078; 07 Jan 1981. *Chem. Abstr.* **1981**, *95*, 7278s.
32. Mohler, H.; Okada, T. *Life Sci.* **1977**, *20*, 2101.
33. Yokoyama, N. US 4,312,870; 26 Jan 1982. *Chem. Abstr.* **1982**, *96*, 18123v.
34. Trapani, G.; Franco, M.; Latrofa, A.; Carotti, A.; Genchi, G.; Serra, M.; Biggio, G.; Liso, G. *Eur. J. Med. Chem.* **1996**, *31*, 575.
35. Hadjipavlon-Litina, D.; Hansch, C. *Chem. Rev.* **1994**, *94*, 1483.
36. Hansch, C.; Leo, A. *Exploring QSAR*; American Chemical Society: Washington, DC, 1995; Vol. 1.
37. Hansch, C.; Leo, A. and Hoeckman, D. *Exploring QSAR*; American Chemical Society: Washington, DC, 1995; Vol. 2.
38. Mickelson, J. W.; Jacobsen, E. J.; Carter, D. B.; Im, H. K.; Im, W. B.; Schreur, P. J. K. D.; Sethy, V. H.; Tang, A. H.; McGee, J. E.; Petke, J. D. *J. Med. Chem.* **1996**, *39*, 4654.
39. Fryer, R. I.; Rios, R.; Zhang, P.; Gu, Z.; Wong, G.; Basile, S. A.; Skolnick, P. *Med. Chem. Res.* **1993**, *3*, 122.
40. Jones, G. B.; Chapman, B. J. *Synthesis* **1995**, 475.
41. Cramer, R. D.; Patterson, D. E.; Bunce, J. D. *J. Am. Chem. Soc.* **1988**, *110*, 5959.
42. *3-D QSAR in Drug Design: Theory, Methods and Applications*; Kubinyi, H., Ed.; Escom: Leiden, 1993.
43. Dunn, W. J. III; Wold, S.; Edlund, U.; Helberg, S. *Quant. Struct.-Act. Relat.* **1984**, *3*, 131.
44. Wold, S.; Johansson, E.; Cocchi, M. In *3D QSAR in Drug Design: Theory, Methods and Applications*; Kubinyi, H., Ed.; Escom: Leiden, 1993; p 523.
45. Cramer, R. D. III; Bunce, J. D.; Patterson, D. E. *Quant. Struct.-Act. Relat.* **1988**, *7*, 18.
46. Thibaut, U. In *3D QSAR in Drug Design: Theory, Methods and Applications*; Kubinyi, H., Ed.; Escom: Leiden, 1993; p 661.
47. Gaillard, P.; Carrupt, P.-A.; Testa, B.; Boudon, A. *J. Comput.-Aided Mol. Des.* **1994**, *8*, 83.
48. Gaillard, P.; Carrupt, P.-A.; Testa, B.; Schambel, P. *J. Med. Chem.* **1996**, *39*, 126.
49. Testa, B.; Carrupt, P.-A.; Gaillard, P.; Billois, F.; Weber, P. *Pharm. Res.* **1996**, *13*, 126.
50. Stewart, J. J. P. *J. Comput.-Aided Mol. Des.* **1990**, *4*, 1.
51. Cramer R. D.; De Priest S. A.; Patterson D. E.; Hecht, P. In *3-D QSAR in Drug Design: Theory, Methods and Applications*; Kubinyi, H., Ed.; Escom: Leiden, 1993; p 443.
52. Allen, M. S.; Tan, Y.-C.; Trudell, M. L.; Narayanan, K.; Schindler, L. R.; Martin, M. J.; Schultz, C.; Hagen, T. J.; Koehler, K. F.; Coddling, P. W.; Skolnick, P.; Cook, J. M. *J. Med. Chem.* **1990**, *33*, 2343.
53. Barnes, A. J.; Ratajczak, H. *J. Mol. Struct.* **1997**, *416*, PAGES.
54. Steiner, T.; Desiraju, G. R. *The Weak Hydrogen Bond: In Structural Chemistry and Biology*; Oxford University: Oxford 1999.
55. Doyon, J. B.; Jain, A. *Org. Lett.* **1999**, *1*, 183.
56. Deerhovanessian, A.; Doyon, J. B.; Jain, A.; Rablen, P. R.; Sapse, A. M. *Org. Lett.* **1999**, *1*, 1360.
57. De Cáceres, M.; Villá, J.; Lozano, J. J.; Sanz, F. *Bioinformatics* (in press).
58. Sanz, F.; Manaut, F.; Rodríguez, J.; Lozoya, E.; López de Briñas, E. *J. Comput.-Aided Mol. Des.* **1993**, *7*, 337.
59. Rodríguez, J.; Manaut, F.; Sanz, F. *J. Comput. Chem.* **1993**, *14*, 922.
60. Schmidt, M. W.; Baldrige, K. K.; Boatz, J. A.; Elbert, S. T.; Gordon, M. S.; Jensen, J. H.; Koseki, S.; Matsunaga, N.; Nguyen, K. A.; Su, S. J.; Windus, T. L.; Dupuis, M.; Montgomery, J. A. *J. Comput. Chem.* **1993**, *14*, 1347.
61. Wold, S.; Eriksson, L. In *Chemometric Methods in Molecular Design*; van de Waterbeemd, H., Ed.; VCH: Weinheim, 1996; p 309.
62. Folkers, G.; Merz, A.; Rognan, D. In *3D QSAR in Drug Design: Theory, Methods and Applications*; Kubinyi, H., Ed.; Escom: Leiden, 1993; p 583.
63. Wold, S. «PLS for Multivariate Linear Modeling» in *ref.* **61**, p 195.
64. Carotti, A.; Altomare, C.; Cellamare, S.; Monforte, A. M.; Bettoni, G.; Loiodice, F.; Tangari, N.; Tortorella, V. *J. Comput.-Aided Mol. Des.* **1995**, *9*, 131.
65. Altomare, C.; Cellamare, S.; Carotti, A.; Barreca, M. L.; Chimirri, A.; Monforte, A.-M.; Gasparrini, F.; Villani, C.; Cirilli, M.; Mazza, F. *Chirality* **1996**, *8*, 556.
66. Altomare, C.; Carrupt, P.-A.; Gaillard, P.; El Tayar, N.; Testa, B.; Carotti, A. *Chem. Res. Toxicol.* **1992**, *5*, 366.
67. Carrieri, A.; Altomare, C.; Barreca, M. L.; Contento, A.; Carotti, A.; Hansch, C. *Il Farmaco* **1994**, *49*, 573.
68. Kneubuhler, S.; Thull, U.; Altomare, C.; Carta, V.; Gaillard, P.; Carrupt, P.; Carotti, A.; Testa, B. *J. Med. Chem.* **1995**, *38*, 3874.
69. Carrieri, A.; Brasili, L.; Leonetti, F.; Pignini, M.; Giannella, M.; Bousquet, P.; Carotti, A. *Bioorg. Med. Chem.* **1997**, *5*, 843.
70. Pignini, M.; Bousquet, P.; Brasili, L.; Carrieri, A.;

Cavagna, R.; Dontenwill, M.; Gentili, F.; Giannella, M.; Leonetti, F.; Piergentili, A.; Quaglia, W.; Carotti, A. *Bioorg. Med. Chem.* **1998**, 6, 2245.

71. Kim, K. H. In *3D QSAR in Drug Design: Theory, Methods and Applications*; Kubinyi, H., Ed.; Escom: Leiden, 1993; p 619.